Springer

Journal of Mechanical Science and Technology 23 (2009) 1751~1759

Journal of Mechanical Science and Technology

www.springerlink.com/content/1738-494x
DOI 10.1007/s12206-009-0409-1

NOx emission characteristics in turbulent hydrogen jet flames with coaxial air †

Hee-Jang Moon*, Yang-Ho Park and Youngbin Yoon

[1]*School of Aerospace and Mechanical Engineering, Korea Aerospace University*
200-1 Hwajeon-dong, Duckyang-gu, Koyang-shi, Kyungki-do 412-791, Korea
[2]*Graduate School, School of Mechanical and Aerospace Engineering, Seoul National University*
College of Engineering Seoul National Univ., Daehak-dong ,Gwanak-gu, Seoul 151-744, Korea
[3]*School of Mechanical and Aerospace Engineering, Seoul National University*
College of Engineering Seoul National Univ., Daehak-dong ,Gwanak-gu, Seoul 151-744, Korea

(Manuscript Received March 4, 2009; Revised March 16, 2009; Accepted March 18, 2009)

Abstract

The characteristics of NOx emissions in pure hydrogen nonpremixed jet flames with coaxial air are analyzed numerically for a wide range of coaxial air conditions. Among the models tested in simple nonpremixed jet flame, the one-half power scaling law could be reproduced only by the Model C using the HO_2/H_2O_2 reaction, implying the importance of chemical nonequilibrium effect. The flame length is reduced significantly by augmenting coaxial air, and could be represented as a function of the ratio of coaxial air to fuel velocity. Predicted EINOx scaling showed a good concordance with experimental data, and the overall one-half power scaling was observed in coaxial flames with Model C when flame residence time was defined with flame volume instead of a cubic of the flame length. Different level of oxygen mass fraction at the stoichiometric surface was observed as coaxial air was increased. These different levels imply that the coaxial air strengthens the nonequilibrium effect.

Keywords: 1/2 power scaling law; Coaxial air; EINOx; Flame length; Nonpremixed flame; Turbulent flow

1. Introduction

Physical effects that impact nitrogen oxides emission in turbulent flame can be classified as flow dynamics, chemistry and radiation when coflow and buoyancy effects are suppressed. The length and shape of the turbulent flame, which are continuously modified by these effects, have tremendous effect on NOx formation [1] especially when the simple turbulent jet flame is subjected to coaxial air.

For the simple turbulent jet flame without coaxial flow, Driscoll et al. [2, 3] showed that the emission index of NOx (EINOx) divided by the flame residence time τ_R, is proportional to the square root of the ratio between fuel jet velocity U_F, and fuel jet diameter D_F. The 1/2 power scaling observed in simple jet flame seems to be an inherent characteristic of NOx emissions and is thought to be related to turbulence-chemistry interaction [4]. Chen and Kollmann [5] showed by numerical analysis that the observed 1/2 power scaling in hydrogen nonpremixed flames is due to a chemical nonequilibrium effect, whereas Schlatter et al. [6] explained by an Eulerian-Lagrangian model that the 1/2 power scaling results from different radical concentration levels controlled by the slow recombination reactions.

These studies on NOx formation in turbulent nonpremixed flames have mostly been focused on simple jet flames without coaxial air. The schematic of coaxial air is shown in Fig. 1. Dahm and Mayman [7]

† This paper was recommended for publication in revised form by Associate Editor Haecheon Choi

*Corresponding author. Tel.: +82 2 300 0118, Fax.: +82 2 3158 3189
E-mail address: hjm@kau.ac.kr

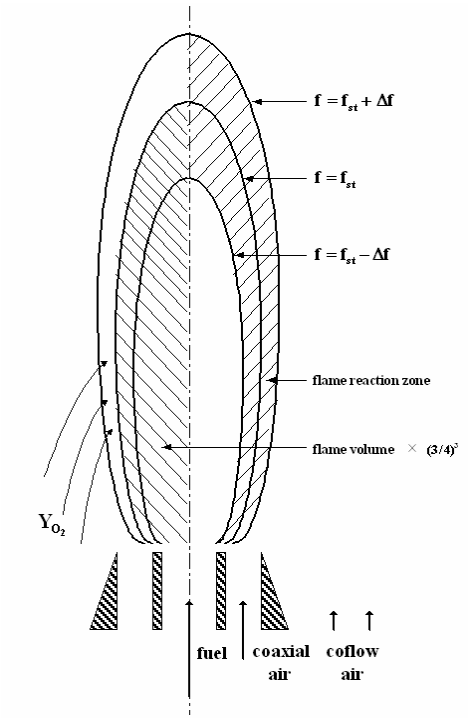

Fig. 1. Schematic of coaxial air flame. Flame volume V_F is defined as $V_F / V_{st} = (4/3)^3$: Barlow and Carter [13].

showed by analysis that coaxial air reduces the amount of entrained air required to dilute the fuel to stoichiometric ratio, decreasing the flame length. Driscoll et al. [2, 3] demonstrated that the effect of coaxial air, which increases mixture homogeneity and shortens the flame length, induces lower NOx emission index than that in the simple jet flames with no coaxial air. More recently, in order to improve the understanding of the physical mechanisms associated with EINOx scaling in coaxial air flames, Kim et al. [8] conducted experiments by varying coaxial air velocity with fixed fuel velocity, and by varying fuel velocity with fixed coaxial air. They found that unlike simple jet flames, EINOx normalized by flame residence time in coaxial air flames is not simply correlated with flame residence time, but rather can be scaled with global strain rate successfully. They also observed through the comparison of undiluted coaxial air flames with He-diluted coaxial air flames that some deviations of EINOx scaling from 1/2-power are due to difference of the radiation effect, because the amount of radiative heat loss that depends on the flame volume is altered depending on the coaxial air velocity.

This paper was motivated by the fact that although coaxial air can become a good concept for NOx reduction technology, the effect of coaxial air has not been examined sufficiently. The specific objectives of the present study are: (1) to test whether chemical nonequilibrium effect has a notable influence on NOx formation characteristics, (2) to test the prediction capability of the proposed combustion model, and (3) to explore the causes of EINOx scaling and its deviation from 1/2-power when coaxial air is increased with fixed U_F.

Our main concern was to analyze the sensitivity of nonequilibrium effect on NOx prediction and EINOx scaling of a turbulent hydrogen coaxial jet flames. After the model test in simple jet flame, flame length and EINOx variation of coaxial air jet flames with respect to U_A variation were studied according to flow conditions. Finally, we attempted to examine the cause of different EINOx scalings.

2. Numerical models

The Favre-averaged Navier-Stokes and $k-\varepsilon$ turbulent equations were solved with the preconditioning method [15]:

$$\Gamma\frac{\partial Q_v}{\partial t}+\frac{\partial E}{\partial x}+\frac{\partial F}{\partial y}+H=\frac{\partial E_v}{\partial x}+\frac{\partial F_v}{\partial y}+H_v+W \quad (1)$$

where Q_v corresponds to $\left\{\tilde{p},\tilde{u},\tilde{v},\tilde{T},\tilde{k},\tilde{\varepsilon},\tilde{g},\tilde{Y}_{N_2},\tilde{Y}^*_{H_2}\right\}^t$ and Γ represents the preconditioning matrix. E, F and H are the x, y directional inviscid flux terms and axisymmetric flux terms, respectively. The subscript v refers to viscous terms, and k and ε are turbulence kinetic energy and dissipation rate of the $k-\varepsilon$ turbulence model, respectively; g and Y_{N_2} mean the variance of mixture fraction and the mass fraction of N_2 respectively. W contains the source terms for $\tilde{T},\tilde{k},\tilde{\varepsilon},\tilde{g}$ and $\tilde{Y}^*_{H_2}$.

Nine species and nineteen reaction steps of Warnatz et al. [10] were used under the partial equilibrium assumption that fast shuffle reactions are in equilibrium. This reaction model is known to predict EINOx scaling correctly in the presumed joint PDF model [9]. The combined variable $Y^*_{H_2}$, for one step chemical reaction model including HO_2/H_2O_2 was expressed by Louis [11] as follows:

$$Y^*_{H_2} = Y_{H_2} + \frac{M_{H_2}}{M_O}Y_O + \frac{3}{2}\frac{M_{H_2}}{M_H}Y_H + \frac{1}{2}\frac{M_{H_2}}{M_{OH}}Y_{OH} - \frac{1}{2}\frac{M_{H_2}}{M_{HO_2}}Y_{HO_2} - \frac{M_{H_2}}{M_{H_2O_2}}Y_{H_2O_2} \quad (2)$$

where M_i and Y_i mean the molecular weight and the mass fraction of species I, respectively. The production term $\dot{\omega}_{H_2}$, for the combined variable $Y^*_{H_2}$, was derived as the summation of relatively linear source terms of third-body recombination reactions as follows:

$$\dot{\omega}^*_{H_2} = -2M_{H_2}(\dot{\omega}_5 + \dot{\omega}_6 + \dot{\omega}_7 + \dot{\omega}_8 + \dot{\omega}_{15}) \quad (3)$$

where $\dot{\omega}_k$ means the k^{th} reaction rate of Warnatz et al.'s nineteen reaction steps [10]. Radicals O, H and OH were determined by the partial equilibrium assumption, and radicals HO_2 and H_2O_2 were obtained by the steady-state assumption. The NO production term was approximated as $\dot{\omega}_{NO} = M_{NO}(2K[N_2][O])$ with the steady-state assumption for radical N and $[NO]/[NO]_{eq} \ll 1$, where $K = 1.84 \times 10^{14}$ exp (-38370/T)cm^3/mol-s. Radiation effect was incorporated via an optically thin limit radiation model [16].

2.1 Presumed joint PDF model and lagrangian IEM model

In the presumed joint PDF model, the state of reaction was determined by three nondimensionalized variables: mixture fraction, $\tilde{f}$, reaction progress variable, $\tilde{r}$, and normalized temperature, $\tilde{T}^*$,

$$\tilde{r} = \frac{\tilde{Y}^*_{H_2} - \tilde{Y}^{*\,u}_{H_2}}{\tilde{Y}^{*\,e}_{H_2} - \tilde{Y}^{*\,u}_{H_2}} \quad \tilde{f} = \frac{\tilde{Z} - \tilde{Z}^a}{\tilde{Z}^f - \tilde{Z}^a} \quad \tilde{T}^* = \frac{\tilde{T} - \tilde{T}^{\min}}{\tilde{T}^{ad} - \tilde{T}^{\min}} \quad (4)$$

where superscripts, a, f, e, u and ad, indicate air, fuel, equilibrium, unburned and adiabatic states, respectively. Z means the mass fraction of element. The PDF for the mixture fraction was assumed to be the beta function. On the other hand, the PDFs of the reaction progress variable and normalized temperature were assumed to be the delta function. Thus, the mean reaction rate was expressed as follows:

$$\tilde{\dot{\omega}}_i = \iiint \dot{\omega}_i(f,r,T^*)P_{beta}(f)P_{delta}(r)P_{delta}(T^*)dfdrdT^* = \int \dot{\omega}(f,\tilde{r},\tilde{T}^*)P_{beta}(f)df \quad (5)$$

where P is the probability density function.

For the Lagrangian IEM model, the Lagrangian equation governing the behavior of a fluid particle was modeled by Villermaux [12] as

$$\frac{d\phi_i}{dt} = \frac{\tilde{\phi}_i - \phi_i}{\tau_{ex}} + \dot{\omega}_i \text{ where } \phi_i = f, Y^*_{H_2}, h \quad (6)$$

$$\tilde{\dot{\omega}}_i = \int \dot{\omega}_i(f,Y^*_{H_2},h)P(Y^*_{H_2}\,|\,f)P(h\,|\,f)P(f)df \quad (7)$$

where h is the enthalpy. The turbulent mixing exchange time τ_{ex} was assumed to be directly proportional to the turbulent characteristic time τ_t, and is modeled as $\tau_{ex} = C_t k/\varepsilon$ where $C_t = 1$. The mean reaction rate, $\tilde{\dot{\omega}}_i$, is obtained from Eq. (7) using the conditional PDFs.

3. EINOx scaling in simple hydrogen jet flames

To verify whether the present numerical models capture the 1/2-power scaling (EINOx / τ_R = $(U_F/D_F)^{1/2}$) of simple jet flames, models' results have been compared to the experimental data of Driscoll et al.[2, 3]. While the inner diameters used for hydrogen fuel nozzles are 1.6, 2.6, and 3.7mm, the coflow air velocity was kept at 0.5m/s for all the cases considered. Grid density of 141 by 98 was selected from the grid dependency test for the computational domain. The discretized equations were solved by a fully implicit time integration method based on LU-relaxation scheme. The convected fluxes were formulated by using a high order accurate TVD scheme based on Koren flux limiter and MUSCL extrapolation method. Three different Models were employed. They are classified by the types of the combination of turbulent combustion models and chemical models: Model A (PDF model without HO_2/H_2O_2 reaction), Model B (IEM model without HO_2/H_2O_2 reaction), and Model C (PDF model with HO_2/H_2O_2 reaction). In simple jet flames, flame residence time is adopted as flow characteristic time closely related to fuel/air mixing time. It means the overall convective time from the fuel inlet to the flame tip and is defined as

$$\tau_R = \frac{Mass\ \ of\ \ flames}{Mass\ \ flow\ \ rate\ \ of\ \ fuel} \propto \frac{\rho V_{NO} f_{sto}}{\dot{m}_{fuel}} \quad (8)$$

where ρ and f_{sto} mean flame density and the stoichiometric value of the fuel. Here it should be emphasized that it is more physical to define NOx formation zone (V_{NO}) with flame reaction zone ($V_{reaction\ zone}$) rather than flame volume (V_f), as sketched in Fig. 1, because NOx is mostly formed in the flame reaction zone near the stoichiometric line.

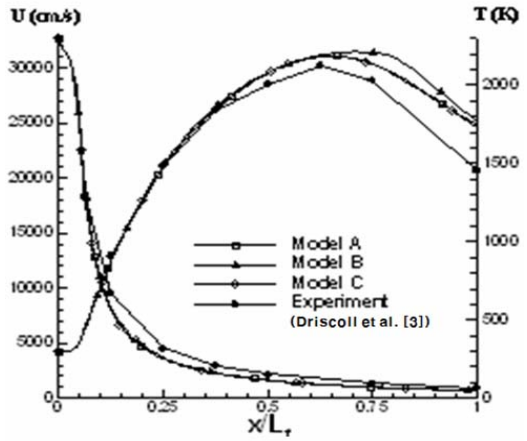

Fig. 2. Comparison of predicted and measured mean flow velocity and mean temperature distributions along the central axis in simple nonpremixed jet flames of Driscoll et al. [3].

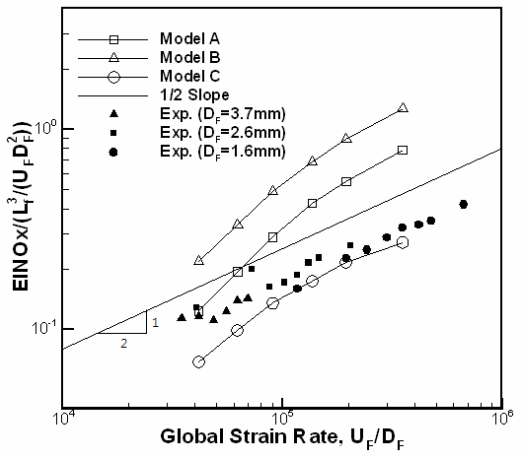

Fig. 3. Comparison of predicted and measured EINOx scaling in simple nonpremixed jet flames of Driscoll et al. [2, 3].

Fortunately, in case of self-similar flames, the flame reaction zone is linearly proportional to the flame volume and two linear relations are also valid: $V_f \propto L_f^3$ and $D_F \propto L_f$ [1-3]. Thus, the flame residence time of simple flame without coaxial air can be simply expressed as

$$\tau_R \propto V_{reaction\ zone}/(D_F^2 U_F) \propto V_f/(D_F^2 U_F) \propto L_f^3/(D_F^2 U_F) \quad (9)$$

However, in jet flame with coaxial air that will be presented in the next section, the relation $V_f \propto L_f^3$ is not valid, and the flame residence time needs to be evaluated directly from the flame volume. The newly defined flame volume is illustrated in Fig. 1. We will remind this at the section dealing with EINOx scaling.

Fig. 2 represents the comparison of measured with predicted mean flow velocity and mean temperature along the centerline of all three models. Though some minor discrepancy between experiments and simulations in mean temperature is observed in the downstream region, all model results closely follow the experimental data. Figure 3 represents the comparison of measured with predicted scaling between EINOx normalized by flame residence time ($EINOx/(L_f^3/U_F D_F^2)$) and global strain rate (U_F/D_F). One can remark that for $U_F/D_F < 10^5$ no notable difference of slope is found among all three models, and that the slope is higher than the 1/2-power scaling of Driscoll et al. [3]. In fact, a higher slope in the low global strain rate region ($U_F/D_F < 10^5$) in which the flame length is relatively long and the fuel diameter is large was also observed in Chen and Kollmann [5]. They attributed the observed higher slopes to the overestimation of the radiative heat loss due to the incompleteness of optically thin radiation model. However, for $U_F/D_F > 10^5$ while Models A and B produce higher slope, Model C not only follows 1/2 slope but also predicts EINOx to an acceptable level. The influences of turbulent combustion models (PDF and IEM) on NOx emissions can be investigated by comparing Model A to Model B in Fig. 3. Although the IEM model overpredicts EINOx than the joint PDF model, both models deliver almost the same tendency of NOx scaling. The quantitative difference is not an important issue since EINOx scaling is not affected by the magnitude of a multiplier in the logarithm scale. Thus, if we focus on the qualitative behavior we can partially conclude that the two turbulent combustion models presented in this study have no effect on NOx formation characteristics as long as the HO_2/H_2O_2 reaction is not taken into account. Model C using the HO_2/H_2O_2 reaction clearly shows the importance of chemical nonequilibrium effect on NOx prediction though the observed 1/2 slope in high global strain rate region ($U_F/D_F < 10^5$). This fact is consistent with that of Chen et al. [4] and Schlatter et al. [6]. Therefore, in the following section Model C will be designated as the test model for the study of nonpremixed jet flame with coaxial air.

4. Results on hydrogen jet flame with coaxial air

4.1 Flame length and EINOx

To examine the effects of coaxial air on NOx for

Table 1. Numerical conditions in the present study. Case I: fixed U_A=10, 20m/s, Case II: fixed U_A/U_F=0.051, 0.068, Case III: fixed U_F=140, 244m/s.

Test Case	U_F [m/s]	U_A [m/s]	U_A/U_F
I	150, 200, 260, 350, 470	**10.0**	0.021~0.066
	160, 200, 260, 350, 470	**20.0**	0.042~0.125
II	140, 180, 230, 295, 380	9.52, 12.2, 15.6, 20.0, 25.8	**0.068**
	140, 180, 230, 300, 390	7.14, 9.18, 11.7, 15.3, 19.9	**0.051**
III	**140**	3, 7, 15, 20, 25	0.021~0.178
	244	3, 9, 15, 20, 25	0.012~0.102

mation, we have performed a numerical analysis for various cases of experiments [8]. The inner diameter and the lip thickness of the fuel nozzle are 3.0 and 0.5mm, respectively. The coaxial air nozzle has a diameter of 15mm and is concentric with the fuel nozzle. Experimental conditions are classified into three groups according to the variations of fuel and coaxial air velocities: Case I (increasing U_F, with U_A fixed), Case II (increasing both U_F and U_A, with U_A/U_F fixed), Case III (increasing U_A, with U_F fixed). Two cases for each group were calculated and the detailed values of U_A and U_F used are shown in Table 1. Coflow air velocity and initial temperature are fixed to 1m/s and 298K, respectively.

Dahm and Mayman [7] showed that in coaxial air flames, the flame length normalized by the diameter of the fuel nozzle can be expressed as a function of the ratio of coaxial air to fuel velocity. Kim et al. [8] experimentally confirmed this relationship between normalized flame lengths and U_A/U_F. Figure 4 represents the comparison of measured and predicted flame lengths. Good agreement with experimental results is shown in the region of the low U_A/U_F close to simple jet flames since $k-\varepsilon$ model constant $C_{\varepsilon 1}$ is modified to be 1.48 so that the flame length can be predicted accurately in the calculation of simple jet flames of Barlow and Carter [13]. However, considerable differences from experimental results are found in the region of the high U_A/U_F, which are thought to be due to the incompleteness of $k-\varepsilon$ model. Figure 4 shows that normalized flame lengths can be represented as a function of U_A/U_F, which is confirmed by Case II with fixed U_A/U_F. Despite different coaxial air and fuel velocities, each simulated value of Case II collapses to a single point indicating the same flame length. However, it is noted that the measured flame lengths do not collapse to a single point. Though not shown in Fig. 4, the normalized flame lengths of Kim

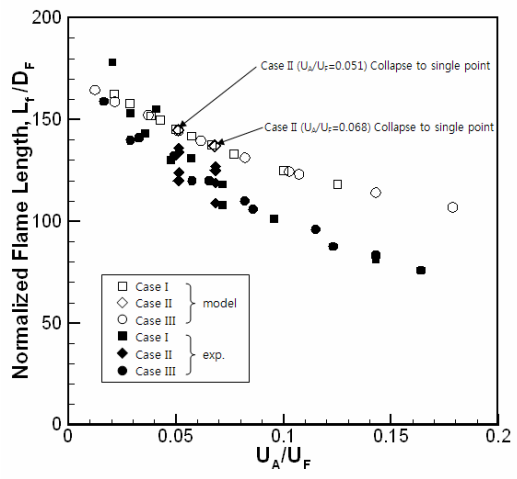

Fig. 4. Comparison of predicted and measured flame lengths in coaxial air flames versus the ratio of coaxial air to fuel velocity. open symbols: present study, filled symbols: Kim et al. [8].

et al. [8] show that for $U_A/U_F > 0.137$, Case II collapses to a single point.

The comparison of predicted with measured EINOx is shown in Fig. 5 as a function of the ratio of coaxial air to fuel velocity. Present modeling exhibits relatively good agreement of EINOx levels with experimental results, although EINOx is rather overestimated. Some overprediction of EINOx may be due to the overestimated flame length of the present numerical calculation as shown in Fig. 4. It is observed that EINOx is substantially reduced with increasing ratio of coaxial air to fuel velocity. Driscoll et al. [2, 3] attributed this considerable NOx reduction to the decrease of the local residence time as well as the reaction zone.

EINOx reduction can be achieved by two processes under the condition of the same nozzle diameter: the decrease of flame volume and the increase of fuel

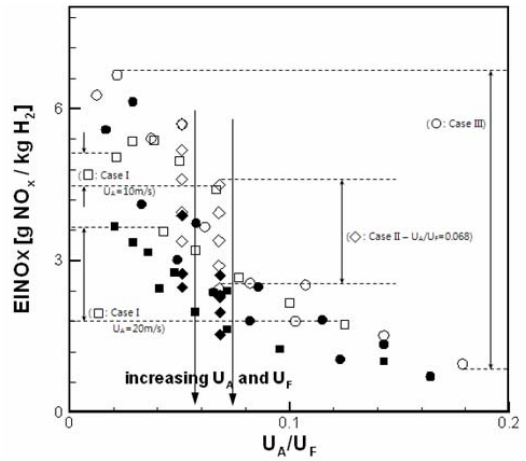

Fig. 5. Comparison of predicted and measured EINOx in coaxial air flames versus the ratio of coaxial air to fuel velocity. Open symbols: present study, filled symbols: Kim et al. [8].

velocity. It is known that the former decreases EINOx by reducing flame reaction zone where EINOx is produced, and the latter by reducing the local residence time for the fuel/air mixture in the high temperature zone. In particular, the latter reason corresponds to simple jet flames because a flame volume is kept constant regardless of the magnitude of fuel velocity. However, in coaxial air flames, two mechanisms can simultaneously work for EINOx reduction, but these effects can be different according to the flow conditions considered. In Case I of Fig. 5, the EINOx range is relatively small compared with Cases II and III. This is because EINOx increased by the growth of the flame volume offsets the EINOx reduced by the increase of fuel velocity. In Case II, the EINOx reduction mainly results from the increase of U_F since the observed normalized flame shapes do not change its form as in simple jet flames, as cited by Moon[14]. In contrast, in Case III, EINOx reduction is maximized as well as its range of variation, and this behavior can be attributed to the decrease of the flame volume because U_F is definitely fixed when U_A changes. Therefore, a much larger reduction of EINOx can be obtained by simple increase of U_A in the coaxial air flames.

Another noteworthy thing for NOx reduction by coaxial air is that the violation of self-similarity law can reduce NOx more significantly than expected under the self-similarity law. Driscoll et al. [2, 3] compared curves of EINOx and L_f^3, and concluded that EINOx reduction is due to the decrease of flame residence time resulting from shorter flame length. However, the decrease of flame residence time cannot be simply explained by the reduced flame length, because the decreasing rate of flame width is not the same as that of flame length in the presence of coaxial air[14]. Especially, EINOx reduction in coaxial air flames (violating self-similarity law) can be larger than expected for simple flames (following self-similar law) since coaxial air flames have a tendency for their nondimensional flame shapes to be thinner as the ratio of coaxial air to fuel velocity increases.

4.2 EINOx scaling of hydrogen jet flames with coaxial air

Unlike in simple diffusion flame analysis, a new definition of flame residence time for EINOx scaling is introduced for coaxial diffusion flame analysis. The fact that a cubic of the flame length cannot be proportional to the flame volume, when coaxial air is in volved, led this study to define the global strain rate and flame residence time as:

$$\text{global strain rate} = (U_F - U_A) / D_F \tag{10}$$

$$\tau_R = V_f / (D_F{}^2 U_F) \tag{11}$$

The flame length and volume in the experiments of Kim et al. [8] were obtained by averaging 20 instantaneous photo images under the assumption that flame shapes are axisymmetric. In this study, the flame length is determined by the empirical relationship of Barlow and Carter [13], i.e., L_f / L_{st} =4/3, where L_{st} is the distance from the fuel inlet to a point where the stoichiometric line intersects with the centerline. Thus, the flame volume V_f is defined as $(4/3)^3$ times of the stoichiometric volume V_{st}, surrounded by the stoichiometric line.

Figs. 6, 7, and 8 show predicted and measured EINOx scalings in coaxial air flames of all three test cases. Large discrepancy between measured and predicted $EINOx / \tau_R$ levels is observed in all cases: I, II, and III. This is because the numerical flame volume calculated by $V_f / V_{st} = (4/3)^3$ is too small compared with real flame volume captured in measurements, so that if a multiplier larger than $(4/3)^3$ is used this discrepancy will disappear. However, the observed quantitative difference is not important because EINOx scaling is not influenced by the magnitude of a multiplier in the logarithm scale. For this reason, the comparison of predicted with measured

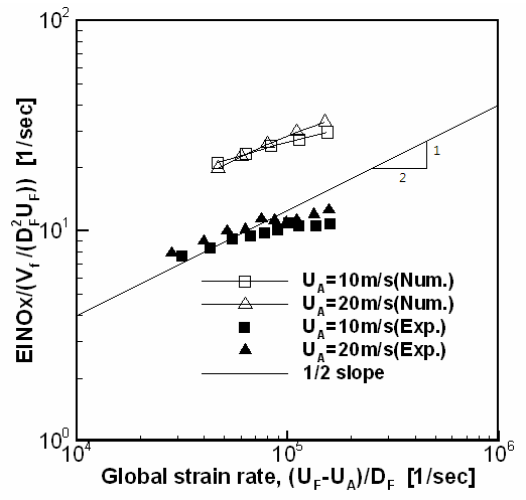

Fig. 6. Comparison of predicted with measured EINOx scalings for Case I with fixed coaxial air velocity. open symbols: present study, filled symbols: Kim et al. [8].

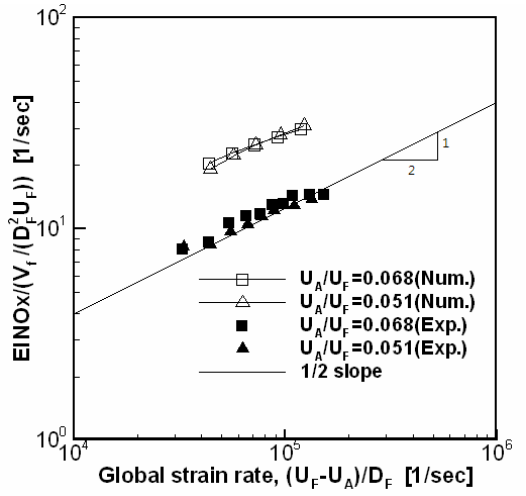

Fig. 7. Comparison of predicted with measured EINOx scalings for Case II with fixed U_A/U_F. open symbols: present study, filled symbols: Kim et al. [8].

EINOx scalings can be qualified, despite the differences of their absolute values.

Predicted EINOx scalings (i.e., slope) almost coincide with measured ones, as shown in Figs 6, 7, and 8 of Cases I, II, and III, respectively. It is noted that EINOx scaling of Cases I and II is quite close to 1/2-power scaling of simple jet flames. Especially, Case II exhibits EINOx scaling closer to 1/2-slope than any other cases. This is because Case II has the most similar characteristics to simple jet flames, as the ratio to coaxial air to fuel velocity is kept constant. However,

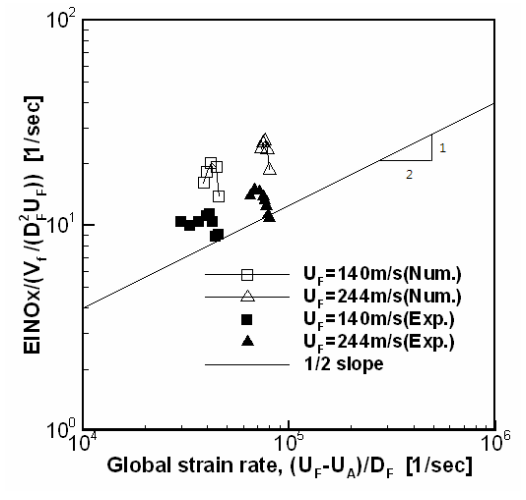

Fig. 8. Comparison of predicted with measured EINOx scalings for Case III with fixed fuel velocity. Open symbols: present study, filled symbols: Kim et al. [8].

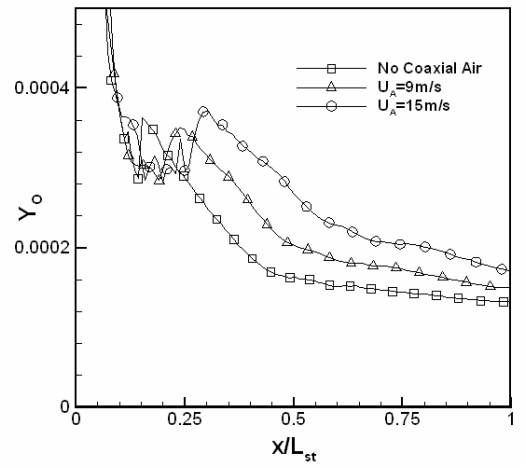

Fig. 9. The variation of mass fraction of oxygen radical at the stoichiometric surface along the downstream direction.

in Case III the effect of coaxial air on NOx emission is significant and notable deviations of EINOx scaling from 1/2-power are observed. The increase of $EINOx/\tau_R$ followed by its subsequent decrease is found in Case III as coaxial air velocity rises. In case III, increase of U_A at fixed U_F decreases global strain rate by the definition, $(U_F-U_A)/D_F$. The increasing part of $EINOx/\tau_R$ results from the rapid decrease of flame residence time, which is caused by a high decreasing rate of the flame volume. This is thought to be due to the fact that fuel-air mixing enhancement due to coaxial air reduces flame length and flame volume. In contrast, the decreasing part of

$EINOx/\tau_R$ is because the flame residence time is diminished at a slower rate as coaxial air velocity further increases. Kim et al. [8] point out that the decrease of $EINOx/\tau_R$ at larger U_A may also be attributed to the flame cooling effect by excess amount of entrained cold air. One can see that even the numerical results grab this phenomenon.

Coaxial air can have an impact on EINOx scaling by changing a variety of physical factors, such as flame residence time, radiation effect and nonequilibrium effect. Especially, Kim et al. [8] pointed out the importance of radiation effect through the comparison of undiluted flame with He-diluted flames. However, radiation effect is beyond the scope of this study so we are rather interested in nonequilibrium effect. In Fig. 9, oxygen mass fraction at the stoichiometric surface along the downstream direction is plotted. The oxygen radical is increased in the downstream region as coaxial air velocity is increased, and these different Y_o levels imply that the coaxial air strengthens the nonequilibrium effect. This is because the augmented turbulent diffusive flux by the coaxial air demonstrated in our companion paper [14] generally leads to a decrease of turbulent characteristic mixing time which has a tremendous effect on nonequilibrium chemistry in the hot reacting zone.

5. Conclusion

The characteristics of NOx emissions in pure hydrogen nonpremixed flames with coaxial air were analyzed numerically for a wide range of coaxial air conditions. Two turbulent combustion models, Lagrange IEM model and joint PDF model were applied to consider turbulence-chemistry interaction either with HO_2/H_2O_2 reaction or without HO_2/H_2O_2 reaction. The three models were first tested in simple nonpremixed flame in order to find the best fitting model with the experiments where the chosen model was used for the analysis of nonpremixed flame with coaxial air. The conclusions from the presented results are as follows.

The model C including HO_2/H_2O_2 reaction reproduces the EINOx 1/2 scaling among three models, and the choice of turbulent combustion models presented in this study has a minor effect on NOx formation. The use of HO_2/H_2O_2 reaction clearly shows the importance of chemical nonequilibrium effect on NOx prediction though the observed 1/2 slope.

The flame length is reduced significantly by coaxial air and can be represented as a function of the ratio of coaxial air to fuel velocity, which is confirmed by the fact that when U_A/U_F is fixed (Case II), flame lengths remain constant despite different coaxial air and fuel velocities. Significant reduction of NOx is obtained by increasing coaxial air unlike in simple jet flames. This is due to the reduced flame reaction zone and flame residence time triggered by the increase of coaxial air. EINOx reduction is maximized as well as its range of variation in Case III, and this behavior can be attributed to the decrease of the flame volume because U_F is definitely fixed when U_A changes. Model C which takes into account the HO_2/H_2O_2 reaction exhibits relatively good agreements of EINOx levels with experimental results, although EINOx is rather overestimated. Some overprediction of EINOx is due to the overestimated flame length of the present numerical calculation as shown in Fig. 4.

Predicted EINOx scalings almost coincide with measured ones, and even the 1/2 power scaling is observed in coaxial flames with Model C when flame residence time is defined with flame volume instead of a cubic of the flame length. Increasing Y_o levels at the stoichiometric surface along the downstream direction is observed when the coaxial air velocity is increased. These different Y_o levels imply that the coaxial air strengthens the nonequilibrium effect. The turbulent combustion model simulation using HO_2/H_2O_2 reaction clearly shows the importance of nonequilibrium effect on EINOx scaling and flame length in both the nonpremixed jet flame with or without coaxial air.

References

[1] S. R. Turns, *Prog. Energy Combust. Sci*., (21) (1990) 281-288.

[2] R.-H. Chen and J. F. Driscoll, *Twenty-Third Symposium (International on Combustion)*, The Combustion Institute, Pittsburgh (1990) 281-288.

[3] J. F. Driscoll, R.-H. Chen and Y. Yoon, *Combust. Flame*, (88) (1992) 37-49.

[4] J.-Y. Chen, W.-C. Chang and M. Koszykowski, *Combust. Sci. and Tech.*, (1995) 505-529.

[5] J.-Y. Chen and W. Kollmann, *Combust. Flame*, (88) (1992) 397-412.

[6] M. Schlatter, J. C. Ferreira, M. Flury and J. Gass, *Twenty-Sixth Symposium (International) on Combustion*, The Combustion Institute, Pittsburgh, (1996) 2215-2222.

[7] W. J. A. Dahm and A. G. Mayman, *AIAA J.*, (28) (1990) 1157-1162.
[8] S.-H. Kim, Y. Yoon and L.-S. Jeung, Nitrogen Oxides Emissions in Turbulent Hydrogen Jet Non-premixed Flames: Effects of Coaxial Air and Flame Radiation, *Proceedings of Combustion Institute*, (28) (2000).
[9] H. J. Moon and R. Borghi, A Lagrangian Based Scalar PDF Method for Turbulent Combustion Models, *KSME International Journal,* (18) (8) (2004) 1470-1478.
[10] J. Warnatz, U. Mass and R. W. Dibble, Combustion, *Springer-Verlag* Berlin Heidelberg, (1996) 67.
[11] J. J. J. Louis, Turbulent Combustion of Coal Gas, *Ph. D. Dissertation*, U. of Twente, (1997).
[12] J. Villermaux, *Encyclopedia of Fluid Mechanics*, (1986) 707-768.
[13] R. S. Barlow and C. D. Carter, *Combust. Flame*, (104) (1996) 288-299.
[14] H. J. Moon, Analysis of Flame Shapes in Turbulent Hydrogen Jet Flames with Coaxial Air, *JMST (*submitted).
[15] Y. Choi and C. L. Merkle, J. *Computational Physics*, (105) (1993) 207-223.
[16] Siegel, Howell, *Thermal Radiation Heat Transfer*, McGraw Hill (1972).

Hee-Jang Moon received his B.S. degree in Aeronautical Engineering from Inha University, Korea in 1986. He then received his M.S. and Doctoral degrees from Universite de Rouen, France in 1988 and 1991, respectively. Dr. Moon is currently a Professor at the School of Aerospace and Mechanical Engineering at Korea Aerospace University in Koyang, Korea. He serves on the Editorial Board of the Korean Society of Propulsion Engineers. His research interests are in the area of turbulent combustion, hybrid rocket combustion and nanofluids.

Youngbin Yoon received his B.S. and M.S. degrees in Aerospace Engineering from Seoul National University, Korea in 1985 and 1987, respectively. He received a Ph.D. degree from the University of Michigan in 1994. Dr. Yoon is currently a professor at the School of Mechanical and Aerospace Engineering in Seoul National University, Korea. He is currently on the Editorial board and executive of ILASS-KOREA. The research areas of Dr. Yoon are liquid rocket injectors, combustion instability and control, ram and gas turbine combustor and laser diagnostics.